AXISYMMETRIC WOUND ROLL MODELS

By

C. Mollamahmutoglu and J. K. Good
Oklahoma State University
USA

ABSTRACT

Axisymmetric wound roll models provide the greatest definition of wound roll internal stresses to date. Simple one dimensional models can provide the user with radial profiles of pressure and circumferential stress as a function of radius. These models later evolved into pseudo two dimensional models where for the first time the impact of web nonuniformities such as thickness and web length could be studied across the web width. These models are described as pseudo two dimensional models because they were a series of the earlier one dimensional models. As such the outputs were limited to the pressure and circumferential stress outputs of one dimensional models but could also be used to predict the shape of the wound roll. Axisymmetric models provide outputs of pressure, circumferential stress, axial stress, and shear stress as a function of radius and cross machine direction location throughout a wound roll. As such these models are capable of describing more types of roll defects than all previous winding models. This paper will focus on the development of a new two dimensional axisymmetric wound roll model based upon a pre-stress formulation. The roll defects that axisymmetric models can be used to analyze will also be discussed.

INTRODUCTION

Winding models have greatly matured since their inception. One dimensional models became essentially mature when Hakiel developed his wound roll model based upon the theory of elasticity [1]. This model was the first to combine all of the important influences that govern the behavior of the winding of elastic web materials. Similar to other one dimensional models Hakiel assumed that the spiral geometry of a web wound onto a core could be replaced by concentric rings of web material. This was the first model that accounted for stiffness of an elastic core and properly treated the web material properties, especially the radial modulus of the wound roll (Er) which is state dependent on pressure or radial strain. This model was a second order differential equation written in terms of radial stress increments and the first and second derivatives of these stress increments

with respect to radius. The radial stress increments were due to the addition of the most recent web layer to the outside of the roll.

$$r^2 \frac{d^2\delta\sigma_r}{dr^2} + 3r\frac{d\delta\sigma_r}{dr} - \left(\frac{E_\theta}{E_r} - 1\right)\delta\sigma_r = 0 \qquad \{1\}$$

The coefficients in this differential equation included a non constant term (the radial modulus) and thus the differential equation could not be solved in closed form. Instead it was solved many times, sometimes as many times as there were layers of web in the wound roll. Each time the equation was solved two boundary conditions were required since the equation was second order. One boundary condition resulted from assumed knowledge of the winding tension from which the radial stress beneath the outer lap could be determined:

$$\delta\sigma_r\big|_{r=s} = -\frac{T_w\big|_{r=s}}{s}h \qquad \{2\}$$

The second boundary condition was based on continuity in deformation at the core. The deformation of the outside of the core had to equal the deformation of the inside of the first layer of the wound roll. This resulted in a derivative boundary condition (radial stress with respect to radius) at the inside of the roll.

$$\left.\frac{d\delta\sigma_r}{dr}\right|_{r=r_c} = \left(\frac{E_\theta}{E_c} - 1 + \nu_{r\theta}\right)\left.\frac{\delta\sigma_r}{r_c}\right|_{r=r_c} \qquad \{3\}$$

Each time the differential equation was solved the increment in radial stress in every web layer was known as a result of winding on the most recent layer. These increments in radial stress were summed within each layer to determine the total pressure. After each lap is added the total radial stress in each layer is used to update the values of the radial modulus (E_r) in each layer. After all layers have been wound onto the roll the final total radial stress as a function of radius is known in the wound roll. Using the equilibrium equation in polar coordinates the circumferential stress can be inferred as a function of radius as well:

$$\sigma_\theta = r\frac{d\sigma_r}{dr} + \sigma_r \qquad \{4\}$$

After executing a model such as Hakiel's a number of times it becomes evident that the winding tension that enters the model through the outer boundary condition is the most influential input parameter. No other input parameter influences the total roll pressures and the circumferential stresses output than the winding tension. Thus it is important in winding models whether they are 1D or 2D models that the winding tension be known accurately and in the case of 2D models that it be distributed correctly across the web width.

PSEUDO 2D WINDING MODELS

Webs are produced and processed by manufacturing methods which cannot produce exact uniformity in thickness and length. Both web thickness and length can vary across the web width. These variations may or may not be persistent in time and thus they may

change down the web length. Both of these imperfections can affect the winding tension across the web width. Again winding tension was the most influential winding parameter found with 1D models and now that parameter is found to vary across the roll width. One dimensional models by definition were incapable of capturing the impact of these nonuniformities on the pressure and circumferential stresses. Based on this need the first pseudo two dimensional wound roll models appeared [2,3]. The adjective *pseudo* is used here in that in both cases these first models were a series of one dimensional models. These models focus on the nonuniform allocation of winding tension across the web width to each the one dimensional models as a function of the outer lap radius across the web width. Hakiel [2] introduced the concept of a relaxation radius r_o. This was the radius of a cylinder of web material in its relaxed state. This cylinder of web was then expanded and allowed to contract onto the outer surface of the wound roll. The total winding tension was the sum of the tensions in the outer laps of the individual sectors represented by the one dimensional winding models. The tension within each sector was dependent on the current outer radius of the roll in a sector, which was calculated by the winding models, and the relaxation radius (r_o) per:

$$T_w = \sum_{i=1}^{n} T_{wi} = \frac{Ebh_{avg}}{n\left(1-\nu^2\right)} \sum_{i=1}^{n} \frac{r_i - r_o}{r_o} \qquad \{4\}$$

In this expression the r_i were the outer radii of each of the one dimensional winding models after the last layer was added. The deformed radius was not a primary output of a one dimensional winding model written as a second order differential equation in radial stress. Given the incremental radial and tangential stresses however the incremental radial strains could be assessed and integrated to produce increments in radial deformation in each lap due to the addition of the most recent lap. These incremental lap deformations could be summed within each lap to produce the total lap deformations which in turn could be used to establish the deformed radial location of all laps.

The value of r_o in expression (4) was iterated until the sum of the web tensions in the individual segments was equal to the applied winding tension. Kedl [3] apportioned the winding tension across the roll width by noting that the wound roll has a constant angular velocity across its width. His first estimate was of the form:

$$T_{wi} = E_\theta \left[1 - \frac{R_{avg}}{R_i}\left(1-\varepsilon_{avg}\right) \right] \quad \text{where } \varepsilon_{avg} = \frac{T_w}{AE_\theta} \qquad \{5\}$$

and R_{avg} is the average radius of the wound roll. The R_i were the outer radii of all the outer laps computed by the one dimensional models. Typically if these first estimates are summed for all of the sector models across the roll width, the sum is less than the total web tension (T_w). This is because the R_i values decrease during the addition of a new layer to the wound roll due to roll deformation. Also the value of R_{avg} is too high because it was computed based upon the undeformed radius of the wound roll. Thus as with Cola and Hakiel's model [2] some iteration is required before the sum of the sector tensions do equal the web tension.

The output of the pseudo two dimensional models developed by Cole and Hakiel [2] and Kedl [3] were limited to the outputs of the one dimensional models they employed. Thus the outputs of these models were the radial and circumferential stresses which were now known as a function of radius and across the web width in sectors represented by the series of one dimensional models. When modeling web thickness variation across the web width the web would be divided into sectors of equal width. Thickness profiles would

then be averaged within the sector to provide a sector web thickness which could be input to the one dimensional winding model for that sector. If these average thicknesses were rearranged the stresses output would be identical but also rearranged. Thus the value of the pseudo two dimensional models was in determining the maximum and minimum pressures and circumferential stresses within a roll and then relating these stresses to associated defects. For instance localized blocking could be predicted due to localized pressures in excess of the blocking pressure. Local yielding of the web could be predicted if the circumferential stresses exceeded the yield stress of the web. An artifact of employing multiple one dimensional models was that the radial continuity of a web layer was not ensured between the sectors. The deformed radial locations of the layers computed were at assumed to exist at the widthwise center of each sector. Hakiel designed a segmented core in which each segment was instrumented with strain gages such that the pressure between the first lap and the core could be monitored throughout the wind. He also developed a device for measuring the radial location of an outer lap across the width of a roll. The segmented core was a deviation from the cores used commercially that are continuous across the roll width. It could be argued that a segmented core was the best means of verifying a pseudo 2D model. As mentioned previously these models provided no assurance of radial continuity of a layer but nor did they assume continuity of the core.

WOUND ROLL PRE-STRESS FORMULATION

A new axisymmetric wound roll model formulation will follow. A key element that must be accommodated is the proper distribution of the web tension across the width of an outer layer whose radius is varying due to web thickness variation. The web tension may vary across the web width as well due to web length nonuniformity.

A Pre-Stress Finite Element Formulation

The concept of a pre-stress type formulation will be introduced. In the wound roll model development the incoming layer has an initial stress called the web line stress. A key feature of a pre-stress type formulation is to incorporate this stress as a source of load for the general roll structure system. The formulation begins with basic concepts of stress and strain relations in linear elasticity:

$$\sigma - \sigma_0 = M\varepsilon$$

Here σ, σ_0, ε are vectors including ordered components of final stress, initial stress and the strain that result from the stress state difference ($\sigma - \sigma_0$) between initial and final configurations respectively. M is the symmetric orthotropic material stiffness matrix which relates the axisymmetric stresses to the corresponding strains. An energy expression which defines the total potential energy of the system will be developed. In the derivation of the total potential energy generally there are two sources. One source is the potential energy produced by the internal forces (stresses) and while the second is the potential of the external forces. There is not an explicit external force for the wound roll winding process. The total potential energy arises only from internal forces. The strain ε which resulted from the stress difference $\sigma - \sigma_0$ will perform work. For a unit volume of the body the elastic potential energy produced by the stress difference can be given as:

$$PE_1 = \frac{1}{2}(\sigma - \sigma_0)^T \varepsilon \qquad \{6\}$$

The factor of ½ results from the linear dependency of the strains on the stress difference. There will also be work performed by the strains ε and the initial stresses σ_0. Since the initial stresses$\sigma_0$existed prior to the development of the strains which resulted from the stress difference there is no factor of ½ :

$$PE_2 = \sigma_0^T \varepsilon \qquad \{7\}$$

The total potential produced in a unit volume will be:

$$TP = \frac{1}{2}(\sigma - \sigma_0)^T \varepsilon + \sigma_0^T \varepsilon \qquad \{8\}$$

and the total potential energy for the entire body can be given by the following volume integral:

$$TPE = \int_V \left(\frac{1}{2}(\sigma - \sigma_0)^T \varepsilon + \sigma_0^T \varepsilon \right) dV \qquad \{9\}$$

This can be solely expressed in terms of the strain and the known initial stress by using constitutive properties which relate the stress difference and the strain (XX). Substituting yields:

$$TPE = \int_V \left(\frac{1}{2}\varepsilon^t M \varepsilon + \sigma_0^t \varepsilon \right) dV \qquad \{10\}$$

where *M* is the symmetric matrix representing orthotropic material behavior. The final energy expression is potential energy of a system with initial stress applied only. Equilibrium will be satisfied when the first variation of the potential energy vanishes with respect to strain. Substituting yields:

$$\delta TPE = \int_V \left(\delta\varepsilon^T M \varepsilon + \delta\varepsilon^T \sigma_0 \right) dV = 0 \qquad \{11\}$$

The finite element method will be used to form a numerical solution of these equations. In the finite element method the body will be divided into sub-bodies with simple geometric characteristics and the unknown variables (displacements herein) will be defined only for the nodes on the boundaries of the sub bodies. These sub bodies are called elements. The total displacement field within the element is then represented by interpolation of the unknown nodal values over the domain of the elements. The same interpolation equations (called shape functions) will be used for all elements. A typical element will have *N* nodes on the boundary of element. Every node will have a certain number of degrees-of-freedom (dof) required by the mathematical model. For example for the wound roll models based on axisymmetrical considerations there will 2 dof for each node of the element in the (*r,z*) coordinate system. These dofs will correspond to the *u* and *w* displacements of each node. The displacement vector within the domain of an element will be defined as:

$$\vec{u}_e = \left[u_e(r,z) \quad w_e(r,z) \right]^T \qquad \{12\}$$

It is assumed that there are *N* representative points or nodes on the boundary of the element. In order to represent the elemental displacement field as an interpolation of the nodal values the unknown vector of nodal displacements is first defined:

$$\vec{u}_e^* = \begin{bmatrix} u_1 & w_1 & ..... & u_N & w_N \end{bmatrix}^T \quad \{13\}$$

The interpolation or shape functions will be denoted as $\phi_i(r,z)$ i=1,…,N, thus the deformation anywhere within the domain of an element can be written in terms of the nodal deformations as:

$$\vec{u}_e = \Phi\ \vec{u}_e^* \quad \{14\}$$

The same shape functions are commonly used to interpolate both the u and w deformations and thus:

$$\Phi = \begin{bmatrix} \phi_1 & 0 & ..... & \phi_N & 0 \\ 0 & \phi_1 & ..... & 0 & \phi_N \end{bmatrix} \quad \{15\}$$

These functions must satisfy some conditions. First the elemental deformation should yield the nodal deformation at the nodal locations. This is ensured by forcing the shape functions to take a value of unity at the node they are associated with and zero at all other nodes. This can be stated mathematically as:

$$\phi_i(r_j, z_j) = \delta_{ij} \text{ for } j=1,\ldots,N \quad \{16\}$$

where δ_{ij} is the Kronecker delta. The second condition is that the shape functions should be as sufficiently smooth as the mathematical model requires. The second condition ensures that derivatives exist in the discrete numerical representation of the mathematical model. Now the strain components can be derived from displacements. Using the differential operator D the element strain vector is:

$$\varepsilon_e = D\vec{u}_e \quad (17)$$

where $$D = \begin{bmatrix} \partial/\partial r & 0 & \partial/\partial z & 1/r \\ 0 & \partial/\partial z & \partial/\partial r & 0 \end{bmatrix}^T \text{ and } \varepsilon_e = \begin{bmatrix} \varepsilon_r & \varepsilon_z & \gamma_{rz} & \varepsilon_\theta \end{bmatrix}^T \quad \{18\}$$

Since the nodal values of deformation are not functions of position the strains can be written in terms of nodal displacements as:

$$\varepsilon_e = (D\Phi)\vec{u}_e^* \quad (19)$$

In this situation the variation of the strain will be simply given with the variation of the nodal displacements:

$$\delta\varepsilon_e = (D\Phi)\delta\vec{u}_e^*,\ \delta\vec{u}_e^* = \begin{bmatrix} \delta u_1 & \delta w_1 & ..... & \delta u_N & \delta w_N \end{bmatrix}^T \quad \{20\}$$

The potential energy expression is written for whole body. Since we are working with finite elements we simply assume that total potential is the sum of the potential energies of the individual elements:

$$\delta W = \sum_{e} \int_{V_e} \delta\varepsilon_e{}^t M_e \varepsilon_e + \delta\varepsilon_e{}^t \sigma_0 dV_e \qquad \{21\}$$

Here for the sake of simplicity every element is assumed to have the same initial stress. If we substitute these discretized strain and its variation into variation of potential energy for a typical element the discretized form of equilibrium is obtained:

$$\delta W = \sum_{e} \delta\left(\vec{u}_e^*\right)^T \left(\int_{V_e} B^T M B dV_e \vec{u}_e^* + \int_{V_e} B^T \sigma_0 dV_e \right) = 0 \qquad \{22\}$$

Here B is the matrix which includes the derivatives of the interpolation functions:

$$B = D\Phi \qquad \{23\}$$

The matrix vector form of elemental equations can be written in terms of element stiffness matrix and element nodal force matrix:

$$\delta W = \sum_{e} \delta\left(\vec{u}_e^*\right)^T \left(K_e \vec{u}_e^* - F_e\right) = 0, \quad K_e = \int_{e} B^T M_e B dV_e, \quad F_e = -\int_{V_e} B^T \sigma_0 dV_e \qquad \{24\}$$

The elements are connected together at boundaries by the nodes. A model of the body can be developed using the general finite element assembly procedure. The global stiffness matrix, global displacement vector and global force vector replace the summation over elements:

$$\delta W = \delta\left(\vec{u}^*\right)^T \left(K\vec{u}^* - F\right) = 0 \qquad \{25\}$$

Finally since the variations are arbitrary, equilibrium can be satisfied by forcing $K\vec{u}^* F$ to vanish. Thus the famous general system of equations for the finite element formulation:

$$K\vec{u}^* = F \qquad \{26\}$$

A Pre-Stress Axisymmetric FEM Wound Roll Model

The general finite element equations for the pre-stress formulation of an axisymmetrical solid body have been written. The axisymmetrical wound roll formulation is based on the accumulation of the web layers as concentric hoops. To solve the complete winding problem as the roll is wound from the core to the final radius requires the solution for the incremental strains and stresses that resulted from the addition of each layer. These increments are summed within each layer to produce the total strains and stresses in that layer. Most web materials have a radial modulus which is dependent on pressure that requires the material properties to be updated as a function of the total pressure after a layer is added. A general geometric view of wound roll model is given in Figure 1. Identical rectangular elements aligned along the z direction for represent a layer.

Since all elements in this case are identical this configuration would correspond to a uniform thickness case. By employing elements with different side heights in the radial direction, a non-uniform web thickness case across z direction can be modeled.

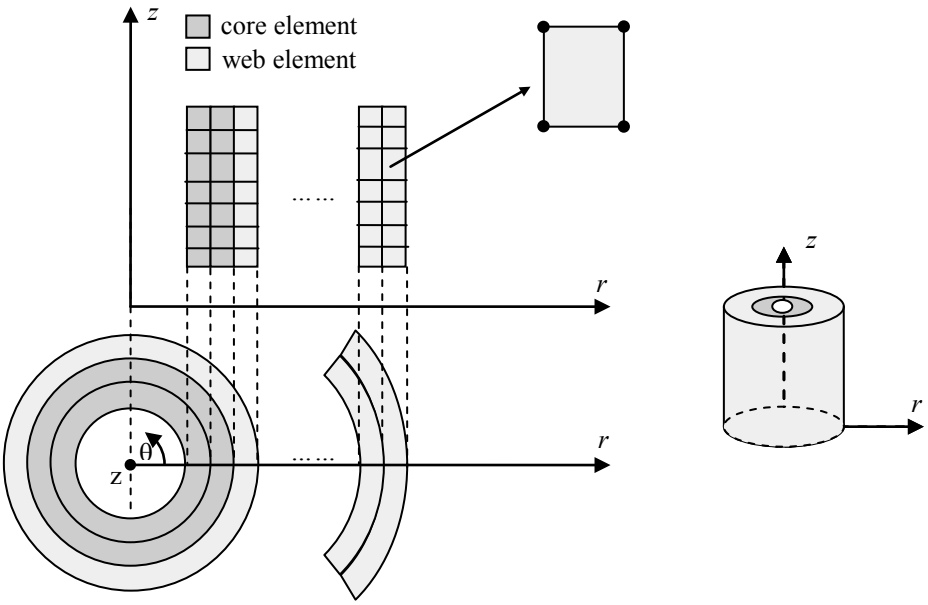

Figure 1 – Modeling of Wound Rolls with Axisymmetric Finite Elements

Most webs are quite thin and the assumption that the stresses are nearly constant throughout the element is reasonable. Quadrilateral elements are optimum in terms of computational time and accuracy and thus were chosen. A typical element has 4 nodes at the corners with linear sides connecting them. Instead of defining the element in the (r,z) coordinate system a natural coordinate system (η,ξ) will be employed which simplifies numerical integration. An isoparametric formulation was employed. This means that the shape functions used to map the element deformations are identical to the functions which define the transformation from original to natural coordinate system. A general quadrilateral element in (r,z) and its mapped counterpart in (η,ξ) coordinates are shown in Figure 2. The related mathematical operations are briefly defined below.

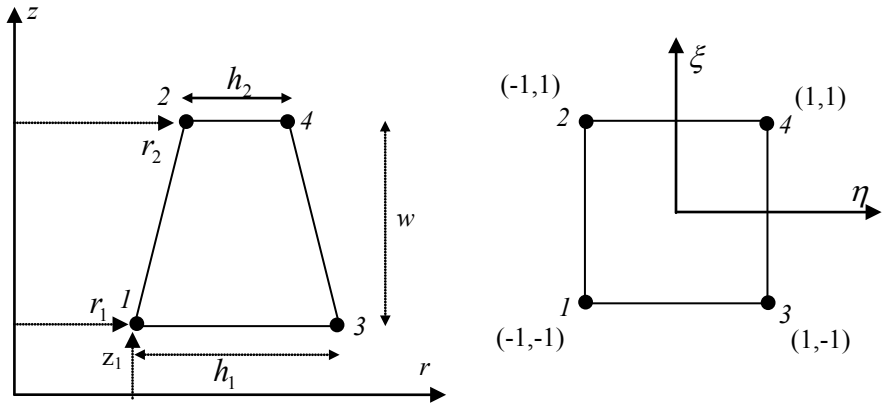

Figure 2 – Actual r-z and Natural ηξ Coordinates for an Axisymmetric Finite Element

The actual coordinates of a point within the element are expressed in terms of nodal coordinates and shape functions. The (r,z) coordinates of the nodes are:

$$\vec{r} = \left[r_1, r_2, r_1 + h_1, r_2 + h_2\right]^T \qquad \{27\}$$

$$\vec{z} = \left[z_1, z_1 + w, z_1, z_1 + w\right]^T \qquad \{28\}$$

The (r,z) coordinates of a point inside the domain of the quadrilateral element are:

$$r(\eta,\xi) = \sum_{j=1}^{4} \vec{r}_j \phi_j(\eta,\xi) \qquad \{29\}$$

$$z(\eta,\xi) = \sum_{j=1}^{4} \vec{z}_j \phi_j(\eta,\xi) \qquad \{30\}$$

For quadrilateral elements the shape functions are easily written in terms of the natural coordinates:

$$\{\Phi\} = \begin{Bmatrix} \phi_1 \\ \phi_2 \\ \phi_3 \\ \phi_4 \end{Bmatrix} = \begin{Bmatrix} \frac{1}{4}(1-\xi)(1-\eta) \\ \frac{1}{4}(1-\xi)(1+\eta) \\ \frac{1}{4}(1+\xi)(1-\eta) \\ \frac{1}{4}(1+\xi)(1+\eta) \end{Bmatrix} \qquad \{31\}$$

With shape functions defined the Jacobian J and its inverse J^{-1} can be formed.

$$\begin{bmatrix} \frac{\partial \phi}{\partial \eta} \\ \frac{\partial \phi}{\partial \xi} \end{bmatrix} = \begin{bmatrix} \frac{\partial r}{\partial \eta} & \frac{\partial z}{\partial \eta} \\ \frac{\partial r}{\partial \xi} & \frac{\partial z}{\partial \xi} \end{bmatrix} \begin{bmatrix} \frac{\partial \phi}{\partial r} \\ \frac{\partial \phi}{\partial z} \end{bmatrix} = [J] \begin{bmatrix} \frac{\partial \phi}{\partial r} \\ \frac{\partial \phi}{\partial z} \end{bmatrix} \quad \{32\}$$

$$J^{-1} \begin{bmatrix} \frac{\partial \phi}{\partial \eta} \\ \frac{\partial \phi}{\partial \xi} \end{bmatrix} = \begin{bmatrix} \frac{4}{(1-\xi)h_1 + (1+\xi)h_2} & 0 \\ \frac{2[(1+\eta)(h_1 - h_2) + 2(r_1 - r_2)]}{w[(1-\xi)h_1 + (1+\xi)h_2]} & \frac{2}{w} \end{bmatrix} \begin{bmatrix} \frac{\partial \phi}{\partial \eta} \\ \frac{\partial \phi}{\partial \xi} \end{bmatrix} = \begin{bmatrix} \frac{\partial \phi}{\partial r} \\ \frac{\partial \phi}{\partial z} \end{bmatrix} \quad \{33\}$$

Components of the inverted Jacobian are used for the transformation of derivatives in the D matrix.

$$D^* = \begin{bmatrix} J_{11}^{-1} \frac{\partial}{\partial \eta} + J_{12}^{-1} \frac{\partial}{\partial \xi} & 0 \\ 0 & J_{21}^{-1} \frac{\partial}{\partial \eta} + J_{22}^{-1} \frac{\partial}{\partial \xi} \\ J_{21}^{-1} \frac{\partial}{\partial \eta} + J_{22}^{-1} \frac{\partial}{\partial \xi} & J_{11}^{-1} \frac{\partial}{\partial \eta} + J_{12}^{-1} \frac{\partial}{\partial \xi} \\ \frac{1}{r(\eta, \xi)} & 0 \end{bmatrix} \quad \{34\}$$

The transformation of the integral for the element stiffness matrix is completed by substituting D^* instead of D and converting the infinitesimal volume element dV_e to the natural coordinates.

$$B = D^* \Phi \quad \{35\}$$

$$dV_e = 2\pi \det[J] r d\eta d\xi \quad \{36\}$$

$$K_e = 2\pi \int_{-1}^{1} \int_{-1}^{1} B^T M_e B \det[J] r d\eta d\xi \quad \{37\}$$

These elemental stiffness terms will be evaluated by employing numerical integration. In this case Gauss Quadrature with 2X2 Gauss points was used for computational efficiency and accuracy. Here the *(p,s)* component of 8x8 axisymmetrical quadrilateral element stiffness matrix is shown:

$$(K_e)_{ps} = 2\pi \sum_{q=1}^{2} \sum_{j=1}^{2} \omega_q \omega_j B^t_{pk(g_q, g_j)} (M_e)_{kl} B_{ls(g_q, g_j)} r(\eta, \xi) \det[J]_{(g_q, g_j)} \quad \{38\}$$

where ω_q and ω_j are the Gauss weights for the q^{th} Gauss point in the ηdirection and j^{th} Gauss point in the ξdirection, respectively. The parenthesizes denote the associated value is calculated at the (g_q, g_j) Gauss point. A similar calculation is carried out for the elemental force vector.

$$F_e = -2\pi \int_{-1}^{1}\int_{-1}^{1} B^t \sigma_0 \det[J] r d\eta d\xi \qquad \{39\}$$

$$(F_e)_p = -2\pi \sum_{q=1}^{2}\sum_{j=1}^{2} \omega_q \omega_j B^t_{pk(g_q,g_j)} (\sigma_0)_k \, r(\eta,\xi) \det[J]_{(g_q,g_j)} \qquad \{40\}$$

Web materials also exhibit state dependent behavior. The radial modulus of elasticity E_r is a function of the radial stress σ_r. One of the most common constitutive relations used is the model of Pfeiffer. He proposed to establish the the following expression for E_r:

$$E_r = K_2(-\sigma_r + K_1) \qquad \{41\}$$

Here K_2 and K_1 are Pfeiffer's material constants which are obtained via stack compression experiments for a particular material. Hakiel employed an expression for E_r of the form:

$$E_r = K_1(1 - e^{\sigma_r / K_2}) \qquad \{42\}$$

Here K_1 and K_2 are different than Pfeiffer's constants for a given web, the point being that the dependency of E_r on radial stress has been modeled using more than one expression. Taking into account Maxwell relations, the elastic compliance matrix C which is the inverse of M can be given explicitly as:

$$\{\varepsilon\} = \begin{Bmatrix} \varepsilon_r \\ \varepsilon_z \\ \gamma_{rz} \\ \varepsilon_\theta \end{Bmatrix} = \begin{Bmatrix} 1/E_r & -\nu_{rz}/E_z & 0 & -\nu_{r\theta}/E_\theta \\ -\nu_{rz}/E_z & 1/E_z & 0 & -\nu_{z\theta}/E_\theta \\ 0 & 0 & 1/G_{rz} & 0 \\ -\nu_{r\theta}/E_\theta & -\nu_{z\theta}/E_\theta & 0 & 1/E_\theta \end{Bmatrix} \begin{Bmatrix} \sigma_r \\ \sigma_z \\ \tau_{rz} \\ \sigma_\theta \end{Bmatrix} = [C]\{\sigma\} \qquad \{43\}$$

$$M = C^{-1} \qquad \{44\}$$

Each finite element will have a different radial modulus E_r depending on the radial stress in that element. This situation makes the problem nonlinear and requires utilizing linearization techniques. Rather than using more complicated and processor time consuming Newton-Raphson methods an ad-hoc approach which is very compatible and sufficient assumes E_r of all elements remain at constant levels during the addition a layer. The system of linear finite element equations can be solved and the incremental stresses due to the addition of the most recent layer can be calculated. Finally the stress state of all elements was updated using the incremental stresses and using the updated stresses E_r for all elements is updated prior to the addition of the next web layer.

This completes the finite element formulation of the problem. Now the appropriate initial stress vector for the simulation of the winding must be defined. Figure 3 shows a typical instance during a winding simulation of a nonuniform thickness web.

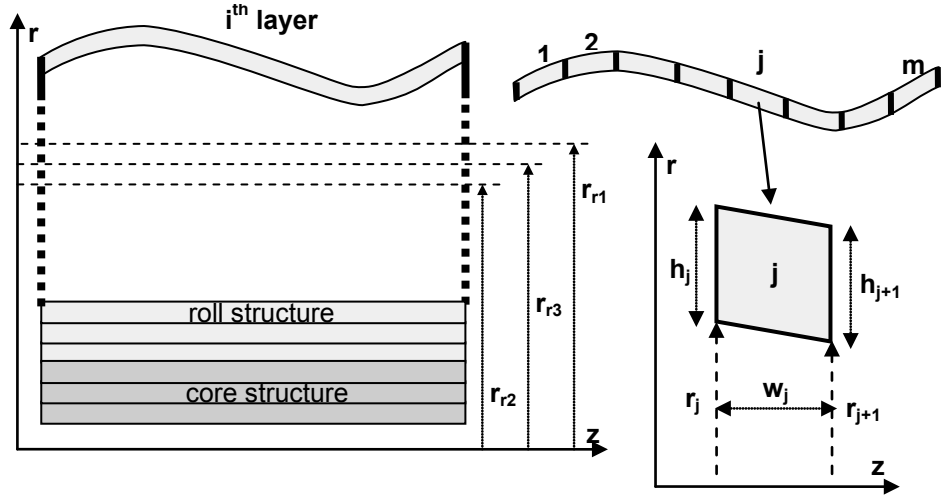

Figure 3 – Treatment of the Outer Lap using a Pre-Stress Formulation

The nonuniform web thickness in the cross machine direction (CMD) results in nonuniform profile in radius across the roll width. This radius profile will vary as the wound roll is wound. Wound rolls may be comprised of hundreds to thousands of layers and if the widthwise web thickness variation persists in the machine direction (MD) large variations in the radius of the outer lap across the roll width can occur. Thus the tension will vary in the outermost layer depending on the CMD position. CMD positions with higher radial profiles should be subject to greater tangential stress and vice versa. In order to simulate this effect in a mechanically consistent manner the notion of a relaxation radius, first coined by Hakiel, will be employed. If it was possible to extract the outer layer from a wound roll and allow it to relax to a stress free state, the radius of the undeformed cylinder of web would be the relaxation radius. Given the relaxation radius for a given roll profile the corresponding strains for all CMD positions can be computed. In a first attempt to calculate the relaxation radius for a given roll profile and web line stress T_w the mechanical equilibrium of the outer winding layer is established:

$$T_w \sum_{j=1}^{m} A_j = \sum_{j=1}^{m} E_{\theta j} \int_0^w \int_{f_1^j(z)}^{f_2^j(z)} \frac{r - r_r}{r_r} dr dz \qquad \{45\}$$

Here A_j and $E_{\theta j}$ are the area and tangential modulus of elasticity for the j^{th} sector, respectively. The integrand is the strain of a radial position in the j^{th} sector so multiplying by $E_{\theta j}$ and integrating over the sector gives the total tangential force contribution of j^{th} sector. A_j and the integral can be expressed explicitly as below:

$$A_j = w \frac{h_j + h_{j+1}}{2} \qquad \{46\}$$

$$\int_0^w \int_{f_1^j(z)}^{f_2^j(z)} \frac{r - r_r}{r_r} dr dz = \frac{w}{6r_r}\left(h_j h_{j+1} + h_j^2 + h_{j+1}^2 + 2r_j h_j + 2r_{j+1} h_{j+1} + r_j h_{j+1} + r_{j+1} h_j\right) - w\left(\frac{h_j + h_{j+1}}{2}\right) \quad \{47\}$$

Here the width of a typical sector is denoted as *w* and it is taken constant. r_r is the unknown relaxation radius which is assumed to satisfy tangential mechanical equilibrium of the winding layer. After algebraic manipulations the relaxation radius r_r is obtained as below:

$$r_r = \frac{\sum_{j=1}^{m} E_{\theta j} Y_j}{T_w \sum_{j=1}^{m} h_j^{ave} + \sum_{j=1}^{m} E_{\theta j} h_j^{ave}} \quad \{48\}$$

$$\text{where } Y_j = \frac{1}{6}\left(h_j h_{j+1} + h_j^2 + h_{j+1}^2 + 2r_j h_j + 2r_{j+1} h_{j+1} + r_j h_{j+1} + r_{j+1} h_j\right)$$

$$\text{and } h_j^{ave} = \frac{h_j + h_{j+1}}{2}$$

This calculated relaxation radius then can be used to calculate the initial stresses of each sector. Here the initial stress vector is obtained and is shown to depend on the calculated relaxation radius as a function of radial position in terms of natural coordinates:

$$(\sigma_0)^j = \begin{bmatrix} 0 & 0 & 0 & E_{\theta j} \dfrac{r_j(\eta,\xi) - r_r}{r_r} \end{bmatrix}^t \quad \{49\}$$

$$\text{where } r_j(\eta,\xi) = \frac{(1+\eta)(1-\xi)h_j + (1+\eta)(1+\xi)h_{j+1} + 2(1-\xi)r_j + 2(1+\xi)r_{j+1}}{4}$$

This initial stress in a vector form is for the j^{th} sector. It can be used in the calculation of corresponding nodal load forces using the elemental force vector:

$$(F_e)_p = -2\pi \sum_{q=1}^{2} \sum_{j=1}^{2} \omega_q \omega_j B^t_{pk(g_q,g_j)} (\sigma_0)_{k(g_q,g_j)} r_{(g_q,g_j)} \det[J]_{(g_q,g_j)} \quad \{50\}$$

This procedure is applied to all elements (sectors) of the winding layer and the resulting elemental load vectors are assembled into a system force vector using the direct stiffness assembly method. The resulting system of equations is solved and the corresponding unknown incremental displacements are obtained for all layers in the roll structure. Incremental strains and stresses are then computed for the addition of the most

recent layer. Since there was no assumed radial compaction of the roll structure when the relaxation radius was computed, the resulting average tangential stress will be lower than the input T_w. This is the result of tension loss. The outer winding layer loses some of its tangential stress as the roll deforms inward beneath it. The degree to which this occurs depends on the radial modulus of the web being wound and the winding tension level. Webs with a high radial modulus will exhibit very little tension loss and the average tangential stress in the outer lap will approach the web line stress T_w.

If it is desired to force the average tangential stress in the outer lap to equal the web line stress T_w a procedure to iterate the relaxation radius of the outer lap is required. The first calculated relaxation radius will be denoted r_{r1}. The first average tangential stress of the outer winding layer calculated via finite element equations will be denoted $T_{\theta 1}$. A smaller relaxation radius than r_{r1} will result in greater average tangential stress so that a second iteration for the relaxation radius, r_{r2}, can be given as:

$$r_{r2} = r_{r1}\frac{T_w}{T_{\theta 1}} \qquad \{51\}$$

After the second relaxation radius r_{r2} is used in the finite element calculations as r_{r1} and solving the resulting equations the average tangential stress $T_{\theta 2}$ for r_{r2} can be obtained. Finally using the first and second approximations for the relaxation radius linear interpolation can be used to solve for the third relaxation radius which would be expected to produce an average tangential stress in the outer layer in the tangential direction equal to the web line stress:

$$r_{r3} = r_{r1} + \frac{T_w - T_{\theta 1}}{T_{\theta 2} - T_{\theta 1}}(r_{r2} - r_{r1}) \qquad \{52\}$$

When the third relaxation radius is input to the finite element code it is found that the average tangential stress is approaching the web line stress (i.e. $\left|T_w - T_{\theta 3}\right| \le c$ and c is typically on the order of 10^{-4}x T_w).

Other Axisymmetric Winding Models

With one axisymmetric winding model described fully other models can be described more easily.

All of these models employ the finite element analysis for solution. These codes were all written as standalone codes, they do not employ commercial solvers. Typically problems that require creation of elements and have state dependent material properties evaluated at intermediate solution steps are not efficiently solved by commercial codes. Of the axisymmetric models reported in the literature Cole and Wickert [4] and Hoffecker and Good [5] have incorporated the use of the small deformation theory and linear strains whereas Arola and von Hertzen [6] incorporated large deformation assumptions. Mollamahmutoglu and Good [7] have conducted a thorough analysis of this topic and found that linear models that accommodate tension loss in the outer lap produce results that are identical to the large deformation models, even for highly compressible web materials such as paper tissues and nonwovens. The Pre_Stress model with no iteration ($T=T_{\theta 1}$) will yield results that are similar to a large deformation model. The Pre_Stress model with iteration ($T=T_{\theta 3}$) will yield results similar to a small deformation model. The final strains, in particular the radial strain ε_r, are of a magnitude such that it might appear that large deformation analyses were required. However the increments in strains in the

layers due to the addition of the most recent layer are small. The largest incremental radial strain is in the outer lap and if the influence of this strain is allowed to decrease the winding tension then the most significant impact of large deformations can be incorporated into a small deformation model.

Both the Wickert and the Arola models do not account for the interaction between the radius profile of the outer lap and the widthwise distribution of winding tension for the next lap. The Hoffecker model does account for this but does so very differently than the prestress model described herein. Hoffecker and Good [5] used a concept similar to that of Cole and Hakiel [2]. The outer lap is formed as a cylinder of constant relaxed radius but with the potential for nonuniform web thickness as shown in Figure 4. Multipoint constraint equations were then used to expand the outer lap cylinder over the outside of the laps that had previously been wound onto the roll.

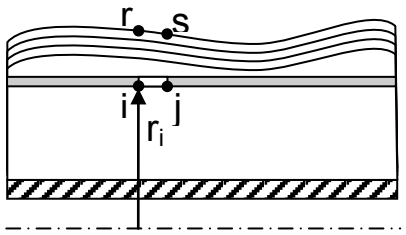

Figure 4 – Hoffecker's Treatment of the Outer Lap

The constraint equations were of the form:

$$\begin{aligned} u_i - u_r &= r_r - r_i \\ u_j - u_s &= r_s - r_j \end{aligned} \qquad \{53\}$$

These equations were enforced using the Lagrangian constraint method. Typically the finite element stiffness matrix for repeating structures is tightly banded about the major diagonal which allows banded solution routines to efficiently solve the set of equations. The Lagrangian constraint equations are added to the set of equations that are solved and destroy the compact bandwidth of the stiffness matrix. This serves to markedly increase solution time. This is one of the benefits of the Pre_Stress method developed herein in that the outer lap is not defined separately. In fact the nodes on the outside of the current lap are common to the nodes on the inside of the new layer being added. This serves to keep the set of equations to be solved as compact as possible. The prestress levels in each element affect only the force vector and no equations of the form of the Lagrangian constraints shown above are required.

BENCHMARKING THE CODES

To benchmark the current axisymmetric codes a comparison with 2D model and test data reported by Cole and Hakiel[2]. The model results are taken from a code developed based on those described by Cole and Hakiel [2]. The test data consists of core pressure data and profilometer data taken to establish the variation in the outer lap radius. The core pressure data was taken on a core composed of ring segments. The segments were composed from aluminum and were 2.54 cm (1 in) wide and had an inside radius of 6.03

cm (2.375 in) and an outside radius of 6.35 cm (2.5)". Each ring segment was supported on pins such that the ring could deform inward axisymmetrically and also transmit the torque required to wind the roll. The ring segments were instrumented with strain gages and these strain measurements allowed the applied core pressure to be inferred. The web used in these tests was a 25.4 cm (10 in) wide polyester film which was nominally 101.6 □m (0.004 in) thick. There were two samples, Case A and B, each having a unique thickness variation across the web width. The traces for the thickness for each Case are shown in Figures 5 and 6. The modeling will employ 20 elements of uniform width and thus the thickness is estimated at 21 positions equally spaced across the web width as shown in Figures 5 and 6.

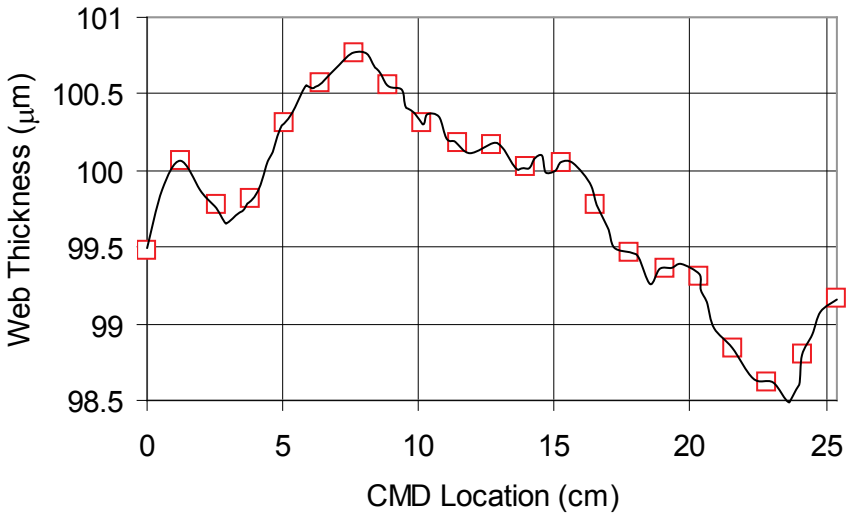

Figure 5 – Hakiel and Cole – Thickness Case A

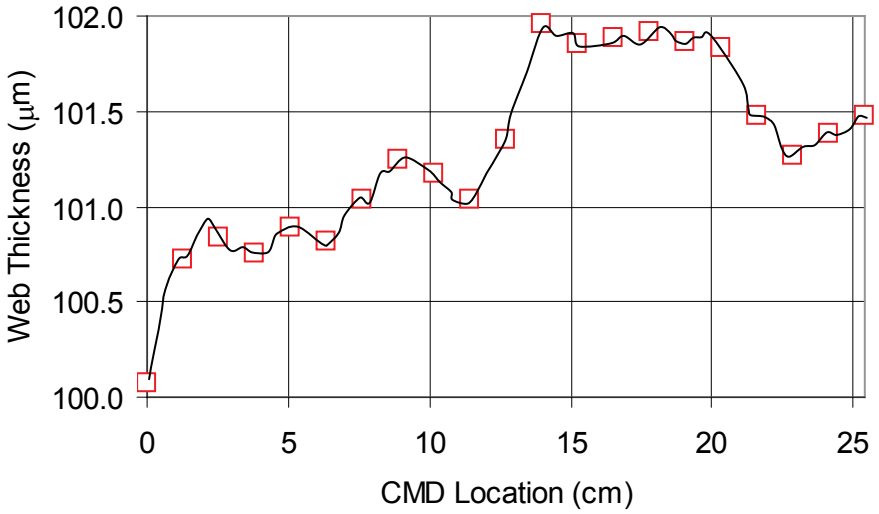

Figure 6 – Hakiel and Cole – Thickness Case B

The remaining parameters required to run the models are given in Table 1. All of these parameters were extracted from Cole and Hakiel [2] except for the in-plane value of Poisson's ratio ($\nu_{\theta z}$) which was assumed and the shear modulus of rigidity G_{rz}. The shear modulus was assumed to be state dependent on radial stress through the radial modulus (E_r) as shown. This assumption was proven valid in other research [8].

Core Diameter	12.7 cm
Finish Roll Diameter	38.1 cm
E_θ, E_z	4.339 GPa
E_r	$E_r = K_1(1 - e^{\sigma_r / K_2})$
K_1	2.4949 GPa
K_2	8.6496 GPa
$\nu_{r\theta}$, ν_{rz}	0.01
$\nu_{\theta z}$	0.3
G_{rz}	$2E_r$
T_w, nominal winding stress	6.863 MPa

Table 1 - Winding Model Input Parameters

Core Pressure Comparison

The model results that will be compared include results from Hakiel and Cole's formulation and the Pre-Stress formulations presented herein. These results will be compared to the core pressure test results presented by Cole and Hakiel [2].

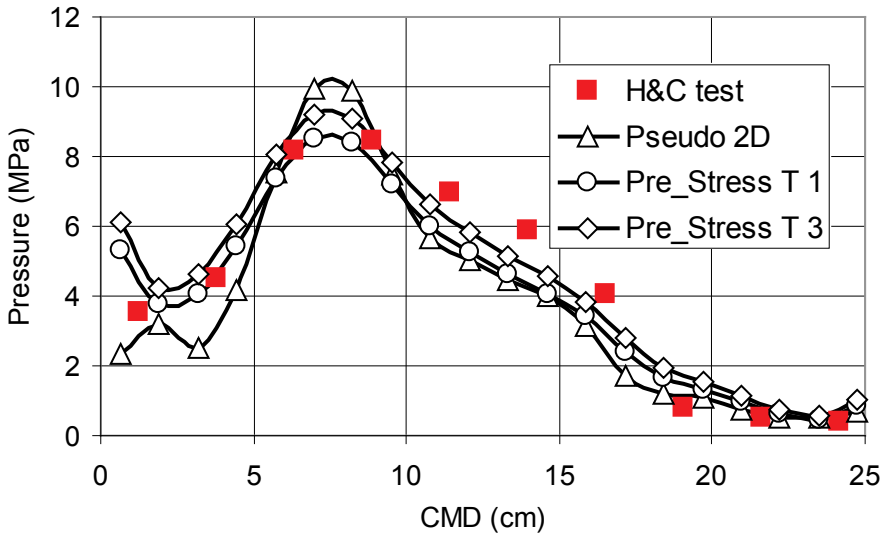

Figure 7 – Core Pressure Comparison – Case A

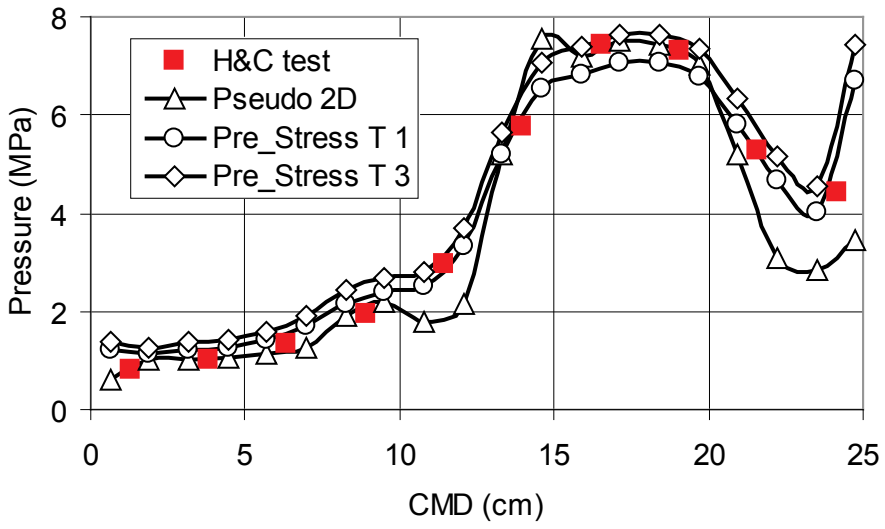

Figure 8 – Core Pressure Comparison – Case B

The Pseudo 2D code developed were developed based upon papers written by Cole and Hakiel [2]. When comparing the core pressures predicted by the models it should be noted that all models compare reasonably well with the core pressure test data. If the core rings that compose the core were deflecting appreciably this comparison would not be

legitimate. This is because the axisymmetric wound roll models assume the core is a cylinder which is continuous over the web width. The Pseudo 2D models assume a segmented core and a segmented web. The reality of the test was a segmented core and a web that was continuous over its width. For Case A all the models yield less pressure than the test values in the 10 to 17 cm range of CMD location. As a measure of performance of the models compared to the test data the mean absolute error was evaluated and the results are shown in Table 2. Overall the axisymmetric Pre-Stress solutions compared the best with the test data. This polyester film has a very high radial modulus and only a small amount of tension loss would be expected. Thus the results from the Pre-Stress $T_{\square 1}$ and $T_{\square 3}$ solutions should not have been appreciably different. It is interesting that the Pseudo 2D model and the axisymmetric Pre_Stress yield results that are so similar given that the model developments are so different.

Model	Pseudo 2D	Pre_Stress $T_{\theta 1}$	Pre_Stress $T_{\theta 3}$
Case A	0.83	0.73	0.72
Case B	0.45	0.31	0.51

Table 2 – Mean Absolute Errors

Outer Lap Comparison

A comparison of the radius variation with respect to the cross machine direction is presented in Figures 9 and 10 for Cases A and B, respectively. The model results all agree quite well with one another. The model results show the same trends as the test data but the range of radius from the model results is nearly twice that of the test data for Case A although there is better agreement for Case B.

It is also interesting to compare the model results in Figures 9 and 10 with the thickness traces presented for Cases A and B in Figures 5 and 6, respectively. Note the trends in measured thickness follow the trends in the outer lap radius predicted by the models. Based upon use of the models alone this might lead to the conclusion that the outer lap radius is entirely dependent on the web thickness variation across the web width. If the trends in measured thickness in Figures 5 and 6 are compared to the measured outer lap radius in Figures 9 and 10 less correlation is apparent. There are some features in the outer lap radius data that appear to repeat with a period close to 2.54 cm, the width of the core rings. It is possible that the independent deformations of the core rings had some impact on the outer lap radius variation across the web width.

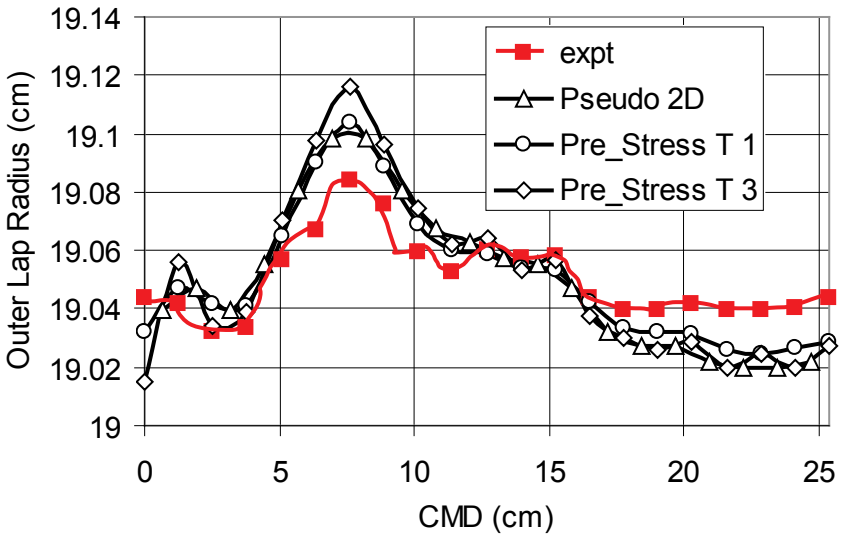

Figure 9 – Outer Lap Radius Comparison – Case A

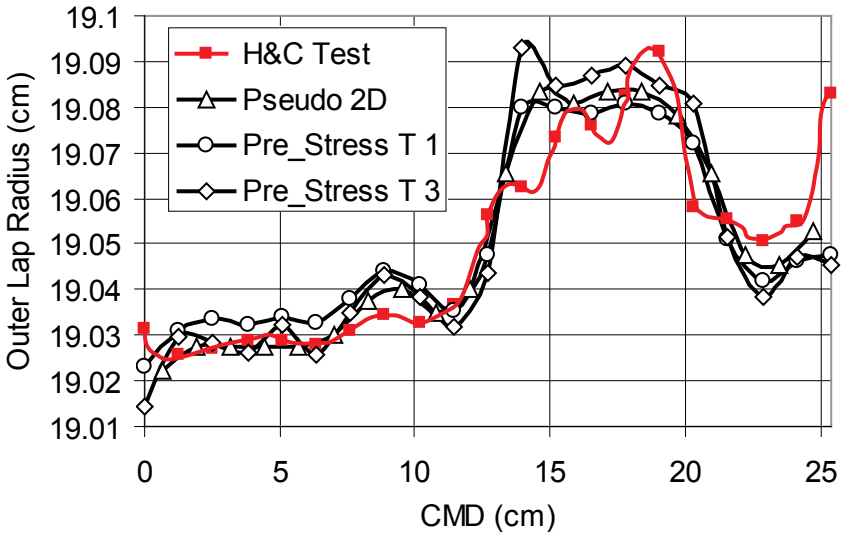

Figure 10 – Outer Lap Radius Comparison – Case B

AXISYMMETRIC STRESSES

The stresses computed by the axisymmetric model include radial, tangential, axial and shear stress components. For Hakilel and Cole's Case B these stresses are shown in Figures 11,12, 13, and 14.

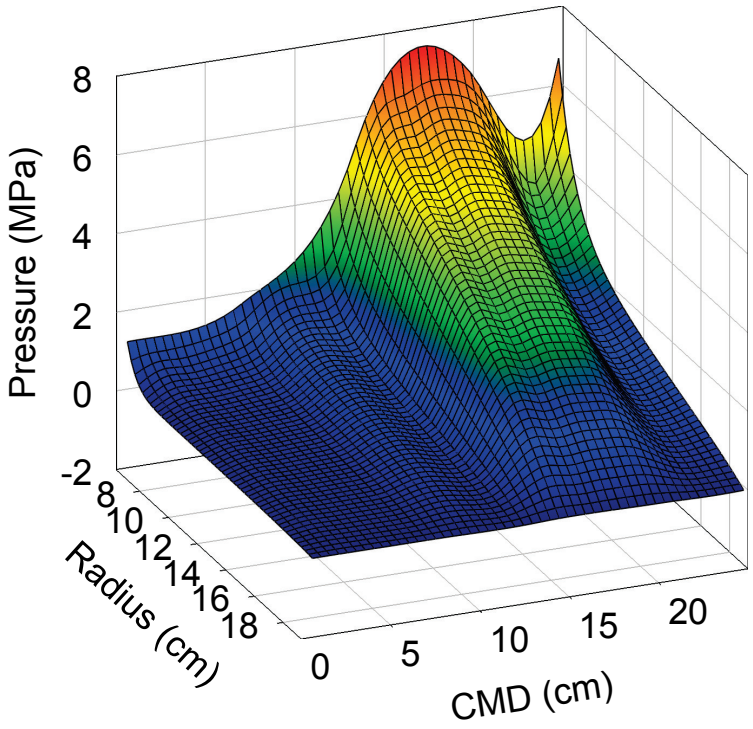

Figure 11 – Pressure ($-\sigma_r$) – Case B

The pressures witnessed by this roll peak at 7.64 MPa (1110 psi). Whether these pressures result in roll and web defects are determined largely by the web surface characteristics and the coatings. Pressures of this magnitude could certainly cause core failures in fiber cores. One of the benefits of an axisymmetric winding model is that a model of an axisymmetric orthotropic core is readily incorporated.

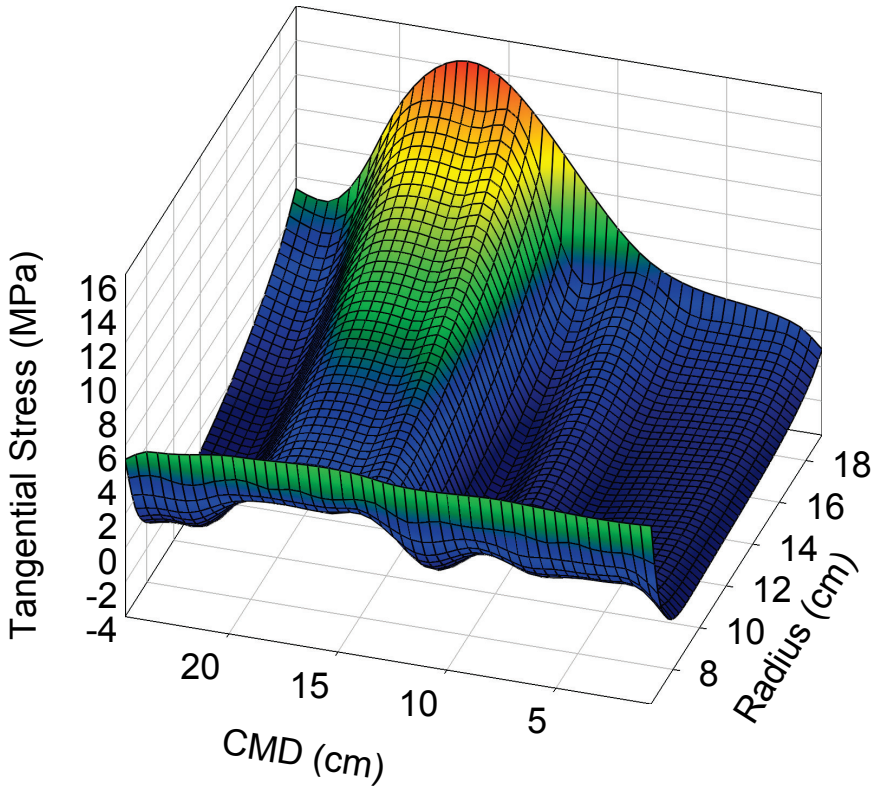

Figure 12 – Tangential Stress – Case B

The peak tangential stress is 15.4 MPa (2240 psi) in the outer lap. The yield stress of polyester is approximately 55 MPa (8000 psi). Thus this stress level may be acceptable as long as the roll is not stored at elevated temperature. The peak tangential stress would have become higher had the roll been wound to a larger radius. The 15.4 MPa peak stress was due to the variation in the outer lap radius that was shown in Figure 10. Had the roll been wound to a larger final radius the variation in the outer lap radius across the roll width would have increased and resulted in an even higher peak tangential stress. Thus these models are useful for determining how large a roll can be wound for given thickness variation prior to subjecting the web to tangential stresses that will induce inelastic deformation or web breaks. Inelastic deformation is undesirable because that deformation will be nonuniform and will peak wherever the tangential stresses peak. When this web is unwound a baggy center will appear.

The axial stresses are shown in Figure 13. Axial stresses cannot be computed using Pseudo 2D models because each of the 1D sector models employ plane stress assumptions (i.e. $\sigma_z=0$). Note for the example given that the peak stresses are negative and are seen in the vicinity of the core. This is a case where the lateral growth of the web is being confined by the core. If the web and the core had properties that were more similar the peak negative axial stresses near the core would decrease and become less negative. Again these models are valuable in deciding what core properties are optimal. Another minimum is seen closer to the surface of the roll. The web width in the free span upstream of the winder is contracted due to the Poisson effect and web tension. After that web enters the wound roll and becomes the outer layer the circumferential stress

decreases as more layers are wound onto the roll, refer to Figure 12. As the tangential stresses decrease the web width attempts to expand in the cross machine direction but is constrained by the frictional contact between layers and hence compressive axial stresses develop. If these stresses become to negative axial buckles or corrugations can appear which may be detrimental to roll quality.

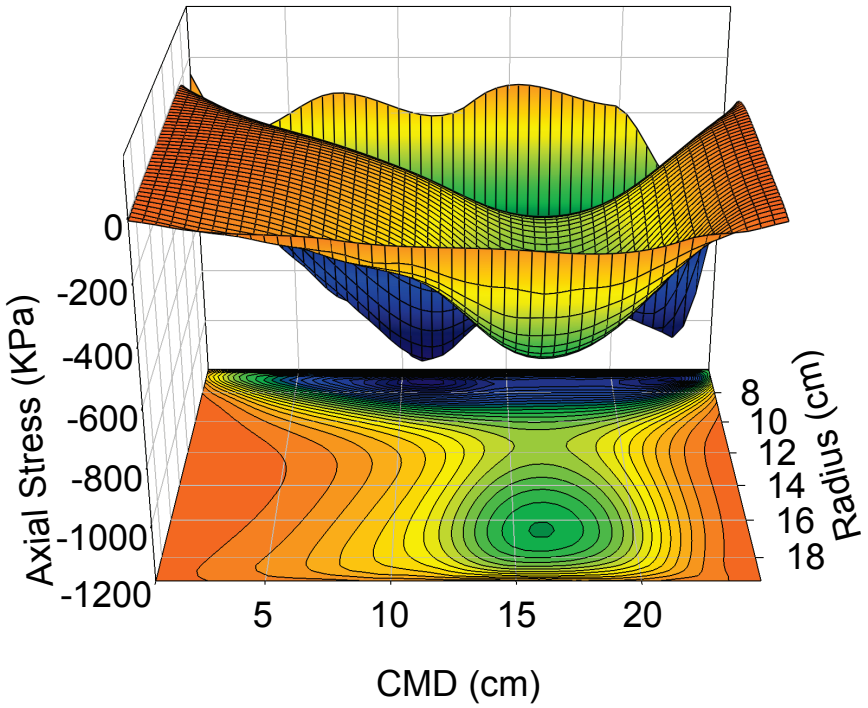

Figure 13 – Axial Stresses – Case B

It is possible to develop 1D winding models using plane strain assumptions that could develop axial stresses and could be incorporated into a Pseudo 2D model. The difficulty is establishing a criterion that would determine when plane stress conditions exist and when plane strain conditions exit. One of the benefits of the axisymmetric finite element wound roll models is that no such assumptions need to be made. Note that in Figure 13 that the axial stresses dissipate to zero at the roll edges (i.e. CMD=0 and 25.4 cm) as dictated by surface equilibrium. Elements which border the edges are subject to near plane stress conditions. Elements in the interior region do attain various levels of axial stress (σ_z) but are not necessarily under plane strain conditions unless the axial strain (ε_z) is zero. Most of the elements in the interior are not in either plane stress or plane strain conditions.

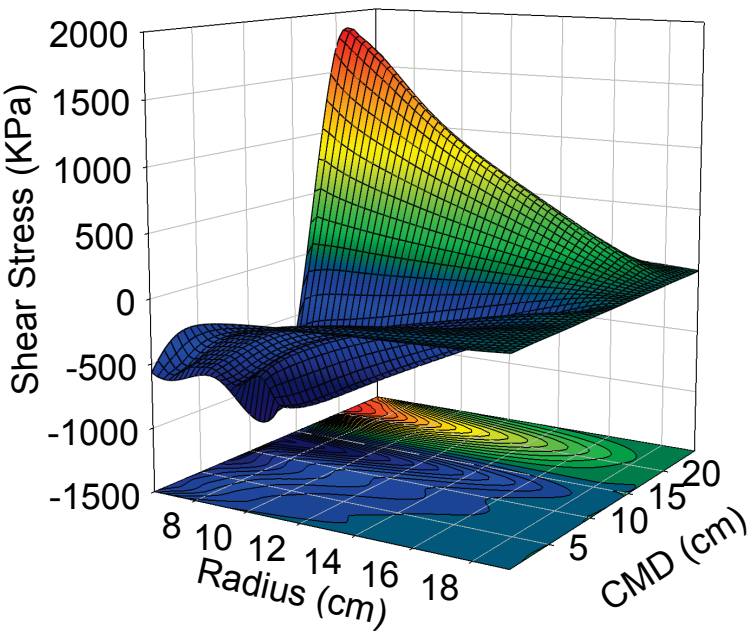

Figure 14 – Shear Stresses – Case B

The shear stresses associated with this example are shown in Figure 14. They too cannot be calculated using the Pseudo 2D models, again due to the plane stress assumption which forces all stress components with an axial or z direction to be zero (i.e. $\sigma_z=0$, $\tau_{rz}=0$). The shear stresses are largest in the vicinity of the core, again due to the vast difference in material properties between the core and the web. They dissipate to near zero levels at the roll edges and at the final lap as is dictated by surface equilibrium.

CONCLUSIONS

The results of Pseudo 2D model and the axisymmetric Pre_Stress model agree very well in terms of core pressure and the variation in radius of the outer lap. Both models compare nicely to the core pressure measurements taken by Cole and Hakiel[2]. Both models capture the trends but not the detail of the measured variation in radius of the outer lap. Additional tests should be performed on web with thickness variation wound on non-segmented cores to determine if the core ring deformations were responsible for the discrepancy.

The Pre_Stress axisymmetric model formulation is optimal because only one solution step is required to achieve results where tension loss is allowed to occur. If one wishes to impose the constraint that the web line stress be equivalent to the average tangential stress in the outer lap then a three step solution process is required.

The stress results from axisymmetric models are important not because they are necessarily more accurate than that of previous models but because the additional stresses computed can allow other types or roll defects to be studied and prevented.

REFERENCES

1. Hakiel, Z., "Nonlinear Model for Wound Roll Stresses," Tappi Journal, Vol. 70, No. 5, May 1987, pp. 113-117.
2. Cole, K.A. and Hakiel, Z., "A Nonlinear Wound Roll Model Accounting for Widthwise Web Thickness Nonuniformities," Proceedings of the Web Handling Symposium, ASME Applied Mechanics Division, AMD-Vol. 149, 1992, pp. 13-24.
3. Kedl, D. M., "Using a Two Dimensional Winding Model to Predict Wound Roll Stresses that Occur due to Circumferential Steps in Core Diameter or to Cross Web Caliper Variation," Proceedings of the First International Conference on Web Handling, Web Handling Research Center, Oklahoma State University, 1991, pp. 99-112.
4. Lee, Y. M. and Wickert, J. A., "Stress Field in Finite Width Axisymmetric Wound Rolls," ASME Journal of Applied Mechanics, Vol. 69, No. 2, 2002, pp 130-138.
5. Hoffecker, P. and Good, J. K., "An Axisymmetric Finite Element Model for Center Winding Webs," Proceedings of the Eighth International Conference on Web Handling, Web Handling Research Center, Oklahoma State University, Stillwater, Oklahoma, 2005.
6. Arola, K. and von Hertzen, R., "Two Dimensional Axisymmetric Winding Model for Finite Deformation," Computational Mechanics, Vol. 40, No. 6, 2007, pp 933-947.
7. Mollamahmutoglu, C. and Good, J.K., "Large Deformation Winding Models," Proceedings of the Tenth International Conference on Web Handling, Web Handling Research Center, Oklahoma State University, 2009.
8. Srinivasan, G., "Diametral Compression of Wound Rolls with State Dependent Material Properties," Master of Science Thesis, Oklahoma State University, 2007.

Axisymmetric Wound Roll Models

C. Mollamahmutoglu & J. K. Good, Oklahoma State University, USA

Name & Affiliation	**Question**
Jon Erik Olsen, SINTEF Materials and Chemistry	What computing times are required in this modeling? What would the benefit of a nip been?
Name & Affiliation	**Answer**
J. K. Good, Oklahoma State University	In the results produced for this paper every layer in the wound roll was modeled. I was probably using more laps than needed but I wanted to ensure that we presented a converged result. What would the benefit of a nip been? We are presenting outer lap tangential stresses here that are varying as a function of the varying outer lap radius across the width of the winding roll. What if that web had instead been wrapping the nip roll prior to entry to the winding roll? Would it have leveled out the winding tension across the web? This is one of the benefits of the nip roll.
Name & Affiliation	**Question**
Tim Walker, T. J. Walker & Associates	With the point you just made, how do you balance out the uniformity from lack of diameter radiations going in with the tension changes you are going to get on the nip that are now pressing on the hard band?
Name & Affiliation	**Answer**
J. K. Good, Oklahoma State University	The CMD locations with higher outer lap radius will experience the highest contact pressures and local nip load levels. A simple wound-on-tension expression would incorporate the nip-induced-tension as a function of the product of the coefficient of friction and the local nip load. So there will be more nip-induced-tension in the CMD locations with high outer lap radius. The result is that winding with the nip will produce a wound roll that is more cylindrical in shape at the expense of inducing high tangential stress and roll pressures in the CMD locations that would have had high outer lap radius. This model can be used to model such behavior. It could be used in nip roll design and to study how nip load should be limited to prevent gage bands from occurring.